

Sensitivity of BEACON to Point Sources of Ultrahigh Energy Neutrinos

**A. Zeolla,^{a,*} J. Alvarez-Muñiz,^b A. Cummings,^a C. Deaconu,^c V. Decoene,^a
K. Hughes,^c R. Krebs,^a A. Ludwig,^{c,d} K. Mulrey,^{e,f} E. Oberla,^c S. Prohira,^g
W. Rodrigues de Carvalho, Jr.,^e A. Romero-Wolf,^{d,h} H. Schoorlemmer,^{f,i}
D. Southall,^c A. G. Vieregg,^c S. A. Wissel^{a,j} and E. Zas^b**

^a*Dept. of Physics, Dept. of Astronomy and Astrophysics, Pennsylvania State University, University Park, PA 16802*

^b*Instituto Galego de Física de Altas Enerxías IGFAE, Universidade de Santiago de Compostela, 15782 Santiago de Compostela, Spain*

^c*Dept. of Physics, Enrico Fermi Institute, Kavli Institute for Cosmological Physics, University of Chicago, Chicago, IL 60637*

^d*Jet Propulsion Laboratory, Pasadena, CA 91109, USA*

^e*Dept. of Astrophysics/IMAPP, Radboud University, Nijmegen, The Netherlands*

^f*Nikhef, Science Park Amsterdam, Amsterdam, The Netherlands*

^g*Dept. of Physics and Astronomy, University of Kansas, Lawrence, KS 66045*

^h*Dept. of Astronomy, California Institute of Technology, Pasadena, CA 91109, USA*

ⁱ*Dept. of High Energy Physic/IMAPP, Radboud University, Nijmegen, The Netherlands*

^j*Physics Dept., California Polytechnic State University, San Luis Obispo, CA 93407*

E-mail: azeolla@psu.edu

The Beamforming Elevated Array for COsmic Neutrinos (BEACON) is a novel detector concept designed to measure the tau neutrino flux above 100 PeV. BEACON consists of multiple radio interferometers placed on mountaintops which search for the radio emission of upgoing extensive air showers created when tau neutrinos skim the Earth. Each interferometer consists of $\mathcal{O}(10)$ low cost, dual-polarized dipole antennas operating in a phased array, which allows for lower trigger thresholds and the directional rejection of noise. A full-scale BEACON will consist of $\mathcal{O}(1000)$ independent antenna arrays and is predicted to be sensitive to the diffuse flux of cosmogenic neutrinos. A Monte Carlo simulation utilizing models of air shower radio emission and the BEACON antennas was developed to predict the sensitivity of BEACON to point sources of tau neutrinos. Any number and configuration of BEACON stations can be simulated. Here, we present the predicted point source sensitivity of a 1,000 station BEACON and compare it to the expected fluence from different possible neutrino sources.

38th International Cosmic Ray Conference (ICRC2023)
26 July - 3 August, 2023
Nagoya, Japan



*Speaker

1. Introduction

Cosmic rays with energies up to 3×10^{20} eV have been detected, but their sources remain unidentified due to their deflection by magnetic fields as they propagate through space. These ultrahigh energy cosmic rays (UHECRs) should create neutrinos as they interact with photons near their source. Neutrinos suffer no deflections as they propagate to the Earth and may therefore be the key to identifying UHECR sources. Suspected sources of UHECRs include many astrophysical transients such as gamma-ray bursts (GRB), tidal disruption events (TDEs), active galactic nuclei (AGN) such as blazars, and binary black hole (BBH) and binary neutron star (BNS) mergers [1].

While astrophysical sources are not expected to produce tau neutrinos, flavor oscillation should result in an astrophysical neutrino flux with an even flavor ratio at Earth, $\nu_e : \nu_\mu : \nu_\tau = 1 : 1 : 1$ [2]. Ultrahigh energy (>100 PeV) tau neutrinos which skim the Earth can produce tau leptons which escape into the atmosphere, decay, and create up-going extensive air showers [3]. Charged particles in the resulting showers are deflected by Earth's magnetic field producing a time-varying current, which in turn causes coherent radio emission; a process known as geomagnetic emission [4]. Ultrahigh energy neutrinos are predicted to have a miniscule flux, so the next generation of detectors must compensate with very large detector volumes.

The Beamforming Elevated Array for COsmic Neutrinos (BEACON) is a novel detector concept designed to detect the radio emission of these up-going extensive air showers and thus measure the flux of ultrahigh energy tau neutrinos. BEACON consists of $O(1000)$ independent phased antenna arrays, each containing $O(10)$ short dipole antennas, placed on mountains around the world. The phased array trigger allows lower trigger thresholds and the directional rejection of noise, while the high elevation site and long propagation length of radio waves provide a very large observation area. Radio antennas are also relatively low cost and can run continuously day or night. A prototype of the BEACON concept, consisting of a single phased array of 4 antennas, is currently deployed in the White Mountains of California. The design and status of the prototype is described in detail in [5].

The BEACON concept has been shown to be sensitive to the predicted diffuse flux of cosmogenic neutrinos [6]. In order to determine BEACON's sensitivity to point sources of astrophysical neutrinos a new Monte Carlo was developed. In these proceedings, we first discuss how point source effective area is calculated and the construction of this Monte Carlo in Section 2. We then show the predicted sensitivity of BEACON to short and long duration transients in Section 3. Lastly, we discuss the implications of these results in Section 4.

2. Monte Carlo

The effective area of an observatory to point sources of neutrinos $A(t, E_\nu, \hat{r})$, derived in [7], is given by

$$A(t, E_\nu, \hat{r}) = \int_{A_g} dA_g (\hat{r} \cdot \hat{x}_E) \Theta(\hat{r} \cdot \hat{x}_E) P_{obs}(t, E_\nu, \hat{r}, \hat{x}_E) \quad (1)$$

where:

t	= the observation time,
E_ν	= the neutrino energy,
\hat{r}	= the vector from the point source to Earth,
A_g	= the geometric area on the surface of the Earth that we integrate over,
\hat{x}_E	= the location of the differential area on the surface of the Earth,
Θ	= the Heaviside step-function,
$P_{obs}(t, E_\nu, \hat{r}, \vec{x}_E)$	= the probability that this event is detected by this observatory.

A Monte Carlo was developed named the **Multiple Antenna Arrays on Mountains Tau Simulation**, or **Marmots**, to numerically solve Eq. 1 and determine the effective area of BEACON. Marmots is based on Tapioca, the point source effective area calculator for ANITA [7], with modifications made to account for the fact that BEACON consists of many independent stations with potentially overlapping observation areas.

Marmots begins by dividing the sky into pixels of equal solid angle, using HEALPix. Each pixel represents a different point source location in the sky in right ascension (α) and declination (δ). The effective area is then calculated for each of these source locations in turn. First, the latitude (ϕ), longitude (λ), altitude a.s.l., field of view (FoV), and orientation relative to East for each station is read in. Any number of stations, placed anywhere globally, can be specified. The elevation and azimuth angle of the source relative to each station is then calculated. Stations which do not view the Earth in the direction of the source are ignored, as they will be unable to detect Earth-skimming neutrinos.

Next, the geometric area on the surface of the Earth in which neutrino exit points are generated, A_g , is calculated. The shower axis for every event is \hat{r} , the vector from the point source at location (α, δ) to the center of the Earth, as we can assume parallel vectors for a distant source. Radio emission is detectable up to some maximum angle away from the shower axis, which we call the maximum view angle. For each station, the ellipsoidal area on Earth in which the station remains within the maximum view angle, as observed from the exit point, is calculated. The total geometric area of all the stations is not necessarily the sum of these areas, as they may overlap. To account for this, the individual areas are sinusoidally-projected onto a 2D plane, conserving their area. The union of these areas, A_g , is then found using the Python module Shapely. Exit points for N events are uniformly generated in the union area, and unprojected into geocentric coordinates. The dot product ($\hat{r} \cdot \hat{x}_E$) is then calculated.

P_{obs} is split into two components: P_{exit} and P_{detect} . P_{exit} is the probability that a tau lepton will exit the Earth. This is a function of energy, as cross-section changes with energy, and exit angle, as this changes the cord-length of the Earth. P_{exit} for each of the N events is calculated by interpolating a lookup-table of NuTauSim [8] results. Energies for the N resulting tau leptons are randomly sampled from a NuTauSim distribution as well. The decay length of each tau lepton is then randomly sampled from an exponential distribution, given the average tau decay length of $E_\tau \times 4.9 \text{ km}/100 \text{ PeV}$. The fraction of energy transferred from each tau to their resulting shower is randomly sampled from distributions generated by PYTHIA [9].

For each station, it is determined which of the N showers have a view angle less than the specified maximum view angle, and decay lengths less than the distance from the exit point to the station, as these are potentially detectable. The peak electric field, \mathcal{E} , for each potentially detectable

event is determined by the same electric field model used by previous BEACON simulations, described here [6]. The model consists of a 4D lookup-table which is interpolated, returning $\mathcal{E}_{lut}(f)$ given the frequency (f), decay altitude, exit zenith angle, and view angle of each event. The lookup-table was generated using a large set of ZHAireS [10] simulations which had fixed shower energies of 100 PeV, and fixed magnetic field magnitudes and directions. Additionally, the distance between decay and detector may differ between the ZHAireS simulations and the events generated by Marmots. To obtain $\mathcal{E}(f)$ for each event i , the $\mathcal{E}_{lut}(f)$ obtained from the look-up tables must be scaled to approximately account for these differences,

$$\mathcal{E}_i(f) = \mathcal{E}_{lut}(f) \times \frac{E_i}{E_{lut}} \times \frac{B_i}{B_{lut}} \times \frac{\sin(\hat{r}_i \times \hat{B}_i)}{\sin(\hat{r}_{lut} \times \hat{B}_{lut})} \times \frac{d_{lut}}{d_i} \quad (2)$$

where:

- E = the shower energy,
- B = the geomagnetic field magnitude,
- $\sin(\hat{r} \times \hat{B})$ = the cross product between the shower axis and geomagnetic field vector,
- d = the distance from decay to detector,

and lut specifies ZHAireS simulation parameters. The geomagnetic field magnitude and direction for each event is determined by IGRF [11] data given the station latitude and longitude.

The gain $G(f, \theta, \phi)$ and impedance Z_A of the short dipoles used in the BEACON prototype have been simulated using XFDTD. The antenna gain in the direction of each shower is first determined by interpolating these results, then $\mathcal{E}(f)$ is converted to peak voltage $V(f)$ using

$$V(f) = N_A \frac{2c}{f} \frac{|Z_L|}{|Z_A + Z_L|} \sqrt{\frac{G(f, \theta, \phi) R_A}{4\pi \eta}} \mathcal{E}(f), \quad (3)$$

where c is the speed of light, Z_L is the impedance at the load, R_A is the resistance of the antenna, and η is the impedance of free space [6]. N_A , the number of antennas in the phased array, is a user input. The full-band peak voltage V_{peak} is found by dividing the full-band into 10 MHz sub-bands, evaluating $V(f)$ at the center frequency of each, and summing. Thermal noise at the receiver is due to a combination of the sky temperature, ground temperature, and system temperature. Sky noise temperature as a function of frequency is modeled using the Dulk parametrization [12]. Ground temperature and system temperature are constants (nominally 290 K and 100 K for BEACON, respectively). Noise power is then converted to noise root-mean-square voltage V_{rms} , which is proportional to $\sqrt{N_A}$ [6].

The SNR of each event is calculated as V_{peak}/V_{rms} . SNRs exceeding a user-chosen value (nominally 5 for BEACON) are deemed to have triggered the station. We are thus left with an array of true/false values for every event for each station. Events which triggered any station have been detected by BEACON, so P_{detect} is the union of all these boolean arrays. Finally, the effective area of the station configuration at each source location (α, δ) is given by

$$A(E_\nu, \alpha, \delta) = \frac{A_g}{N} \sum_{i=1}^N (\hat{r}_i \cdot \hat{x}_{i,E}) P_{i,exit} P_{i,detect}. \quad (4)$$

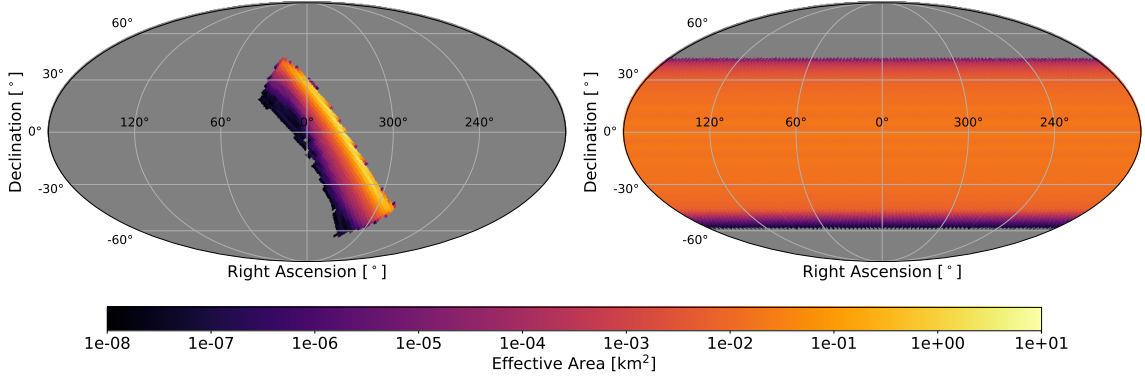


Figure 1: The instantaneous (left) and diurnally-averaged (right) effective area predicted by Marmots for a 100-station BEACON to 1 EeV tau neutrinos. The stations are spaced 3 km apart, along a line of equal longitude, and centered on the location of the current prototype ($\phi = 37.5893^\circ$, $\lambda = -118.2376^\circ$, $h = 3.851$ km). The stations face East with a 120° FoV, and contain 10 phased antennas each.

3. Results

Marmots was run for 11 energies, 10^{16} to 10^{21} eV in half-decade bins. The station configuration consisted of 100 stations spaced 3 km apart, along a line of equal longitude. The line was centered on the location of the current prototype ($\phi = 37.5893^\circ$, $\lambda = -118.2376^\circ$). The altitude of each station was set to be that of the prototype (3.851 km), and they all faced due East with a 120° FoV. The number of phased antennas in each station (N_A) was chosen to be 10. The calculated instantaneous effective area of this configuration to 1 EeV tau neutrinos is shown on the left of Fig. 1. As the Earth rotates, the sources in view of BEACON will change. The diurnally-averaged effective area of BEACON can be calculated by incrementally rotating the instantaneous effective area by a few degrees in right ascension, summing, and then dividing by the total number of rotations. This result is shown on the right of Fig. 1.

The sensitivity of a detector to an all-flavor $dN_\nu/d\mathcal{E}_\nu \propto E_\nu^{-2}$ neutrino flux is given by

$$E_\nu^2 \phi_\nu = \frac{2.44}{0.5 \ln(10)} \frac{3 E_\nu}{A(E_\nu)}, \quad (5)$$

where the 3 accounts for the fact that it is an all-flavor flux and we only have an effective area to tau neutrinos, and $2.44/[0.5 \ln(10)]$ is the 90% unified confidence level of detecting zero candidate or background events over a half-decade of energy [13].

For short-duration transients, $A(E_\nu)$ in Eq. 5 is found from the instantaneous effective area of BEACON $A(E_\nu, \alpha, \delta)$ (left of Fig. 1). Using the maximum value of $A(E_\nu, \alpha, \delta)$ gives us BEACON's peak sensitivity to short duration transients. This peak occurs due East—where the antenna gain and geomagnetic effect are maximized—and just below the horizon. The peak sensitivity for a 100-station BEACON to short-duration transients is shown in Fig. 2. Also shown is the sensitivity scaled by a factor of 10, to approximate the sensitivity of a 1000-station BEACON. These curves are compared to predicted neutrino fluences from BNS mergers at 5 Mpc [14], as well as from sGRB at 40 Mpc, viewed on-axis, during two phases: extended (EE) and prompt emission [15].

For long-duration transients, $A(E_\nu)$ in Eq. 5 is found using the diurnally-averaged effective area of BEACON $A(E_\nu, \alpha, \delta)$ (right of Fig. 1). The average of $A(E_\nu, \alpha, \delta)$ from a declination angle

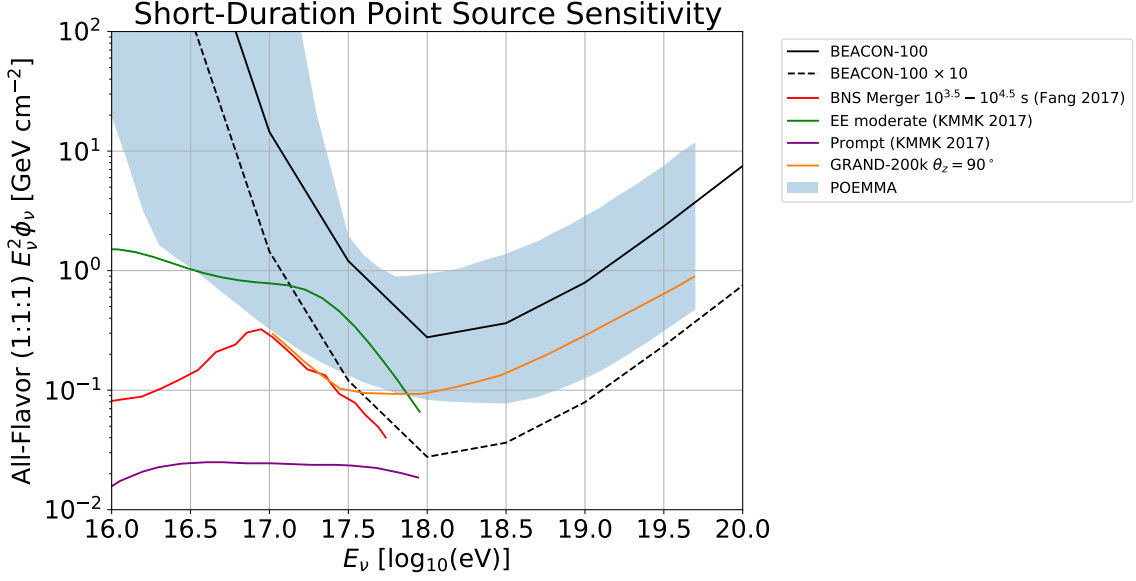


Figure 2: The sensitivity of a 100-station BEACON to short-duration transients calculated using Eq. 5 and the peak instantaneous effective area predicted by Marmots. Also shown is this sensitivity scaled by a factor of 10 as an approximation of the sensitivity of a 1000-station BEACON. These are compared to a model of the all-flavor fluence from a stable millisecond magnetar $10^{3.5} - 10^{4.5}$ s after a BNS merger, scaled to a source distance of 5 Mpc [14], and the modeled all-flavor fluence from sGRB viewed on-axis, scaled to a distance of 40 Mpc, during two phases: extended (EE) and prompt emission [15]. The sensitivity of the experiments GRAND-200k, at a zenith angle of 90° [16], and POEMMA [17] are also plotted.

of -50° to 30° is used for $A(E_\nu)$. The result for a 100-station BEACON is shown in Fig. 3. Once again, the sensitivity of 1000 stations has been estimated by scaling the 100 station result. Also plotted are the predicted neutrino fluences from BNS mergers to stable millisecond magnetars on two time scales, $10^{4.5} - 10^{5.5}$ s and $10^{5.5} - 10^{6.5}$ s, at a source distance of 5 Mpc [14].

4. Conclusions

We see from Fig. 1 that while the instantaneous effective area of BEACON peaks along a narrow band (the horizon), BEACON can still observe a large portion of the sky as the Earth rotates. From Fig. 2, we see that 1000 stations would be able to probe extended emission sGRB neutrino fluence models. With additional stations, the prompt emission phase could also be probed. We see in Fig. 3 that 1000 stations can probe BNS merger neutrino fluence models at 5 Mpc.

In the future, topography will be incorporated into Marmots in order to observe its effect. Surrounding mountains could be a potential interaction target for Earth-skimming tau neutrinos, increasing the effective area. Time-domain electric fields and the antenna response will also be incorporated, allowing us to fully simulate neutrino waveforms. More station configurations will also be tested, as changing the configuration can change the instantaneous and diurnally-averaged effective area, as well as the sky coverage. By allowing any configuration to be input, Marmots will be helpful in selecting future sites for BEACON stations.

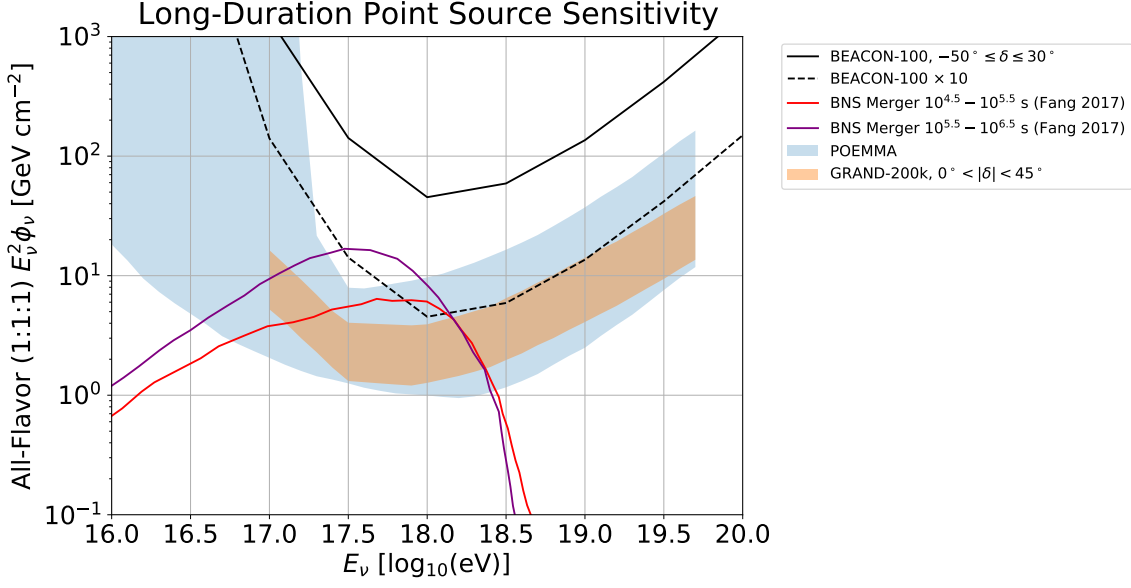


Figure 3: The sensitivity of a 100-station BEACON to long-duration transients calculated using Eq. 5 and the diurnally-averaged effective area predicted by Marmots, averaged over the declination range $-50^\circ \leq \delta \leq 30^\circ$. Also shown is this sensitivity scaled by a factor of 10 as an approximation of the sensitivity of a 1000-station BEACON. These are compared to the modeled all-flavor fluence from a stable millisecond magnetar $10^{4.5} - 10^{5.5}$ s and $10^{5.5} - 10^{6.5}$ s after a BNS merger, scaled to a source distance of 5 Mpc [14]. The sensitivity of the experiments GRAND-200k, over the declination range $0^\circ < |\delta| < 45^\circ$ [16], and POEMMA [17] are also plotted.

This work is supported by NSF Awards # 2033500, 1752922, 1607555, PHY-2012980, and DGE-1746045 as well as the Sloan Foundation, the RSCA, the Bill and Linda Frost Fund at the California Polytechnic State University, and NASA (support through JPL and Caltech as well as Award # 80NSSC18K0231). This work is also funded by Xunta de Galicia (CIGUS Network of Res. Centers & Consolidación ED431C-2021/22 and ED431F-2022/15), MCIN/AEI PID2019-105544GB-I00 - Spain, and European Union ERDF. We thank the NSF-funded White Mountain Research Station for their support. Computing resources were provided by the University of Chicago Research Computing Center.

References

- [1] M. Ackermann et al., *Astrophysics Uniquely Enabled by Observations of High-Energy Cosmic Neutrinos*, *Bull. Am. Astron. Soc.* **51** (2019) 185 [1903.04334].
- [2] J.F. Beacom, N.F. Bell, D. Hooper, S. Pakvasa and T.J. Weiler, *Measuring flavor ratios of high-energy astrophysical neutrinos*, *Phys. Rev. D* **68** (2003) 093005.
- [3] E. Zas, *Neutrino detection with inclined air showers*, *New Journal of Physics* **7** (2005) 130.
- [4] F.G. Schröder, *Radio detection of cosmic-ray air showers and high-energy neutrinos*, *Progress in Particle and Nuclear Physics* **93** (2017) 1–68.

- [5] D. Southall et al., *Design and Initial Performance of the Prototype for the BEACON Instrument for Detection of Ultrahigh Energy Particles*, *NIM-A* **1048** (2023) 167889 [2206.09660].
- [6] S. Wissel et al., *Prospects for high-elevation radio detection of >100 PeV tau neutrinos*, *JCAP* **11** (2020) 065 [2004.12718].
- [7] ANITA collaboration, *Analysis of a tau neutrino origin for the near-horizon air shower events observed by the fourth flight of the Antarctic Impulsive Transient Antenna*, *Phys. Rev. D* **105** (2022) 042001 [2112.07069].
- [8] J. Alvarez-Muñiz, W.R. Carvalho, A.L. Cummings, K. Payet, A. Romero-Wolf, H. Schoorlemmer et al., *Comprehensive approach to tau-lepton production by high-energy tau neutrinos propagating through the Earth*, *Phys. Rev. D* **97** (2018) 023021 [1707.00334].
- [9] T. Sjöstrand, S. Ask, J.R. Christiansen, R. Corke, N. Desai, P. Ilten et al., *An introduction to PYTHIA 8.2*, *Comput. Phys. Commun.* **191** (2015) 159 [1410.3012].
- [10] J. Alvarez-Muñiz, W.R. Carvalho and E. Zas, *Monte carlo simulations of radio pulses in atmospheric showers using ZHAireS*, *Astroparticle Physics* **35** (2012) 325.
- [11] P. Alken, E. Thébaud, C. Beggan et al., *International geomagnetic reference field: the thirteenth generation*, *Earth Planets Space* **73** (2021) 49.
- [12] G. Dulk, W. Erickson, R. Manning and J.-L. Bougeret, *Calibration of low-frequency radio telescopes using the galactic background radiation*, <http://dx.doi.org/10.1051/0004-6361:20000006> **365** (2001) .
- [13] G.J. Feldman and R.D. Cousins, *A Unified approach to the classical statistical analysis of small signals*, *Phys. Rev. D* **57** (1998) 3873 [physics/9711021].
- [14] K. Fang and B.D. Metzger, *High-Energy Neutrinos from Millisecond Magnetars formed from the Merger of Binary Neutron Stars*, *Astrophys. J.* **849** (2017) 153 [1707.04263].
- [15] S.S. Kimura, K. Murase, P. Mészáros and K. Kiuchi, *High-Energy Neutrino Emission from Short Gamma-Ray Bursts: Prospects for Coincident Detection with Gravitational Waves*, *Astrophys. J. Lett.* **848** (2017) L4 [1708.07075].
- [16] GRAND collaboration, *The Giant Radio Array for Neutrino Detection (GRAND) project*, *PoS ICRC2021* (2021) 1181 [2108.00032].
- [17] T.M. Venters, M.H. Reno, J.F. Krizmanic, L.A. Anchordoqui, C. Guépin and A.V. Olinto, *POEMMA's Target of Opportunity Sensitivity to Cosmic Neutrino Transient Sources*, *Phys. Rev. D* **102** (2020) 123013 [1906.07209].